Science of the Total Environment 550 (2016) 297–308

Contents lists available at ScienceDirect

Science of the Total Environment

journal homepage: www.elsevier.com/locate/scitotenv

Profiling microbial community in a watershed heavily contaminated by an active antimony (Sb) mine in Southwest China

Weimin Sun [a,b], Enzong Xiao [a,c], Yiran Dong [d], Song Tang [e], Valdis Krumins [f], Zengping Ning [a], Min Sun [a,c], Yanlong Zhao [g], Shiliang Wu [g], Tangfu Xiao [a,*]

[a] State Key Laboratory of Environmental Geochemistry, Chinese Academy of Sciences, Guiyang 550002, PR China
[b] Department of Biochemistry and Microbiology, Rutgers University, New Brunswick, NJ 08901, USA
[c] University of Chinese Academy of Sciences, Beijing 100049, PR China
[d] Department of Geology, University of Illinois—Urbana Champaign, Urbana, IL 61801, USA
[e] School of Environment and Sustainability, University of Saskatchewan, Saskatoon, SK S7N 5B3, Canada
[f] Department of Environmental Sciences, Rutgers University, New Brunswick, NJ 08901, USA
[g] Water Resources Protection Bureau of Pearl River Water Resources Commission, Guangzhou 510611, PR China

HIGHLIGHTS

- We characterized the microbial communities of a Sb-contaminated watershed.
- We studied the interaction between microorganisms and different Sb fractions.
- Many bacterial phylotypes were positively correlated with different Sb fractions.
- CCA demonstrated that chemical parameters structured the microbial communities.

GRAPHICAL ABSTRACT

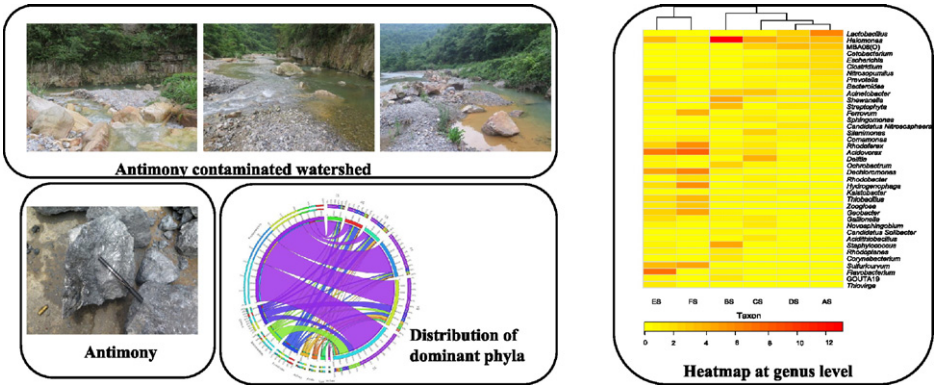

ARTICLE INFO

Article history:
Received 23 November 2015
Received in revised form 14 January 2016
Accepted 14 January 2016
Available online 25 January 2016

Editor: D. Barcelo

Keywords:
Antimony contamination
Microbial community analysis
Sb-metabolizing bacteria
Statistical analysis
Bioremediation

ABSTRACT

Located in Southwest China, the Chahe watershed has been severely contaminated by upstream active antimony (Sb) mines. The extremely high concentrations of Sb make the Chahe watershed an excellent model to elucidate the response of indigenous microbial activities within a severe Sb-contaminated environment. In this study, water and surface sediments from six locations in the Chahe watershed with different levels of Sb contamination were analyzed. Illumina sequencing of 16S rRNA amplicons revealed more than 40 phyla from the domain Bacteria and 2 phyla from the domain Archaea. Sequences assigned to the genera *Flavobacterium*, *Sulfuricurvum*, *Halomonas*, *Shewanella*, *Lactobacillus*, *Acinetobacter*, and *Geobacter* demonstrated high relative abundances in all sequencing libraries. Spearman's rank correlations indicated that a number of microbial phylotypes were positively correlated with different speciation of Sb, suggesting potential roles of these phylotypes in microbial Sb cycling. Canonical correspondence analysis further demonstrated that geochemical parameters, including water temperature, pH, total Fe, sulfate, aqueous Sb, and Eh, significantly structured the overall microbial community in Chahe watershed samples. Our findings offer a direct and reliable reference to the diversity of microbial

* Corresponding author at: 99 Lincheng Road West, Guiyang 550081, Guizhou Province, PR China.
E-mail address: xiaotangfu@vip.gyig.ac.cn (T. Xiao).

http://dx.doi.org/10.1016/j.scitotenv.2016.01.090

communities in the presence of extremely high Sb concentrations, and may have potential implications for *in situ* bioremediation strategies of Sb contaminated sites.

1. Introduction

Antimony (Sb) is a naturally occurring toxic metalloid belonging to Group 15 of the periodic table that has been classified as a suspected carcinogen (Gebel, 1997; Hammel et al., 2000) as well as a pollutant of priority interest by the US Environmental Protection Agency (USEPA). The USEPA sets its maximum contaminant level (MCL) for Sb in drinking water at 6 μg/L (USEPA, 1979), while the Council of the European Communities (1976) and China (He et al., 2012) sets 5 μg/L as the maximum admissible concentration of Sb in drinking water. Sb and its compounds can be released into surface water, soils, and sediments by natural processes or by anthropogenic activities such as industry or mining (He et al., 2012; Okkenhaug et al., 2011), leading to a range of environmental and human health concerns. Wastewaters produced from Sb mining activities contaminated the surrounding aquatic environment, resulting in high concentration of Sb in both water and sediment in Goesdorf, Luxembourg (Filella et al., 2009). The elevated concentration of Sb in contaminated water can reach up to hundreds to thousand times of nature water (<1 μg/L) (Filella et al., 2002), which pose adverse impact on local ecosystem (He et al., 2012; Wang et al., 2011). Moreover, Sb can have far-reaching impacts because of its strong mobility and complexation reactions in water and sediments (Fawcett and Jamieson, 2011; Filella, 2011). Sb contamination has been reported to pose health risks to exposed populations globally (Migon et al., 1995; Villarroel et al., 2006), especially in China, which is the largest Sb producer in the world with 114 Sb mines and approximately 90% of the world's production (He et al., 2012). Human exposure to Sb is primarily through contaminated water and food (Belzile et al., 2011), causing damage to the liver, lungs and cardiovascular system (Feng et al., 2013; Gebel, 1997). Environmental exposure to antimony from contaminated sites is a suspected cause of morbidity in some localities in China. He and Yang reported the potential role of the elevated Sb levels in increased incidence of dermatitis and pneumoconiosis in residents living near the Xikuangshan (XKS) Sb mine in Hunan Province (He and Yang, 1999).

Despite the toxicity of Sb, a wide range of microorganisms can survive and thrive in Sb-contaminated environments. Microbial transformations of Sb that promote precipitation and immobilization *in situ* are promising strategies for remediation of contaminated sediments and waters. Microbial Sb cycling is mainly mediated through reduction, oxidation and methylation. Luo et al. utilized metagenomics and real-time PCR to characterize the microbial gene expression in arsenic (As) and Sb in As- and Sb-contaminated soils (Luo et al., 2014). They showed that the distribution, diversity, and abundance of functional genes related to As and Sb cycling (*e.g.*, *arsC*, *arrA*, *aioA*, and *arsB*) were positively correlated with both As and Sb concentrations (Luo et al., 2014). These observations suggest that dynamic Sb biogeochemical cycling may occur in contaminated sites. It is unclear whether these reports of microbial Sb oxidation, reduction and methylation are related to respiration or detoxification. However, high abundances of several bacterial genera including *Sphingomonas*, *Caulobacter*, *Janthinobacterium*, *Geobacter*, *Rhodoferax*, and *Sulfuricurvum*, have been found in Sb-rich mine tailings (Majzlan et al., 2011), suggesting tolerance, if not utilization, of Sb.

Although Sb and As have some physical, toxicological and chemical similarities (Gebel, 1997), our current knowledge of Sb biotransformation is still very limited in comparison to the extensive studies on the genetics and biochemistry of microbial As cycling. It is still unclear how microbial populations shift in response to long-term Sb pollution and what geochemical factors affect the microbial community composition in Sb-contaminated environments. Dissolved and adsorbed metal(loid)s in sediments are easily exchangeable and generally thought to be the most bioaccessible fractions (Filella et al., 2007; Savonina et al., 2012), whereas metal(loid)s occluded in minerals are believed to be less bioaccessible and relatively immobile (Okkenhaug et al., 2011; Savonina et al., 2012). Unfortunately, previous reports of Sb effects on microbial communities in aquatic environments have failed to distinguish different Sb sequential extraction fractions (Majzlan et al., 2011). The lack of comprehensive understanding of these linkages has thus been a barrier to progress in natural attenuation and/or bioremediation of Sb pollution.

The Chahe watershed (Fig. 1), located in Guizhou Province, Southwest China, provides an excellent opportunity to investigate the interaction between microorganisms and elevated Sb concentrations in sediments and surface water. Two major rivers, the Dajiagou River and the Chahe River, comprise the watershed. These rivers are located downstream of a large active Sb mine. Extensive mining has resulted in high concentrations of metal(loid)s, particularly Sb, being discharged

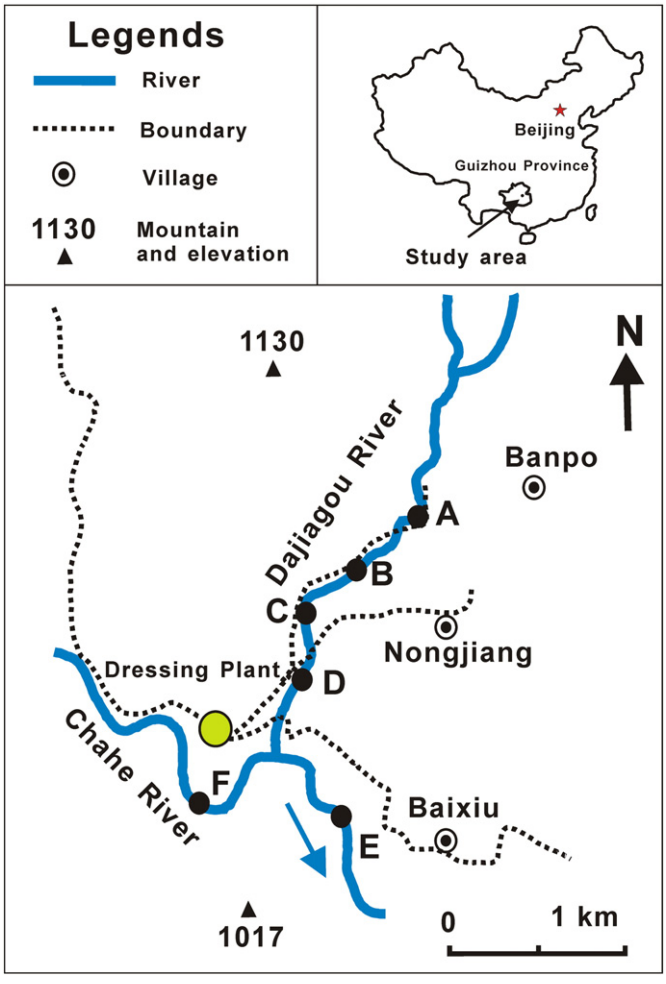

Fig. 1. Map of locations of six sampling sites (A–F) in the Chahe watershed. The Sb mining area and dressing plant are also illustrated. Sediment samples are denoted as AS-FS and water samples are denoted as AW-FW corresponding to their respective sampling sites. Boundary stands for township boundary. The blue arrow indicated water flow. Insert map shows the general map of China. The insert map of China and map of Chahe watershed were created by AutoCAD 2014 (Autodesk, Mill Valley, USA).

into the rivers, with concentrations of Sb reaching 3248 μg/L in surface water and 16,071 mg/kg in sediments as measured in the current study. Developing efficient bioremediation strategies requires comprehensive understanding of the geochemical factors influencing community structures and the metabolic potentials of the indigenous microbial communities. For this reason, we integrated molecular approaches and geochemical analytical methods to decipher the microbial community structure in response to elevated Sb concentrations. More specifically, our aims were to (1) characterize spatial dynamics of the microbial community structure and composition in response to different Sb contamination gradients; and (2) to study the interaction and correlation between microorganisms and different Sb fractions in sediments as well as other environmental physiochemical variables.

2. Materials and methods

2.1. Site locations and sample collection

Representative sampling locations were selected for geochemical and microbial community analyses. Because the riverbed of Dajiagou River is mainly composed of big rock, only four locations in Dajiagou River were found to have accumulated sufficient fine-grained sediment for further chemical and microbiological analyses (Fig. 1). Two other representative sampling locations from Chahe River were selected as well: One site (site E) in Chahe River downstream of its confluence with Dajiagou River, and one site (site F) within Chahe River that was impacted by the upstream ore dressing plant. At each sampling site, water (denoted as AW-FW) and sediment (AS-FS) samples were collected in October, 2013. For water samples, about 5 L of water from each sampling site was immediately filtered through a 0.45 μm sterile membrane (Jinjing, Shanghai, China). The filtered water was preserved with ultrapure 37% HCl to prevent Fe(II) oxidation and stored at 4 °C in darkness for subsequent geochemical analysis. Approximately 300 g of surface sediment was collected by skimming the upper 1–2 cm sediment with a wide mouth container. Samples were immediately transferred to sterile plastic bottles and were immediately stored at −20 °C until further analysis.

2.2. Geochemical parameters

Water quality parameters including temperature (T), pH, salinity (Sal), conductivity (Con), total dissolved solid (TDS) and redox potential (Eh) were measured onsite by a calibrated HACH HQ30d pH meter (HACH, Loveland, CO, USA). Major and trace elements in water samples were measured by inductively coupled plasma-optical emission spectrometry (ICP-OES) (Vista MPX, Varian, USA) and inductively coupled plasma mass spectrometry (ICP-MS) (Agilent, 7700×, Santa Clara, CA, USA), respectively. Anions and total organic carbon (TOC) were measured by ion chromatography (Dionex, ICS-90, Sunnyvale, CA, USA) and a high TOC II analyzer (Elementar, Hanau, Germany), respectively.

Sediment samples were air-dried and thoroughly ground using a mortar and pestle before passing through a 200-mesh sieve. To measure pH in sediments, 4 g of dry sediment was mixed with 10 mL distilled water, shaken for 5 min, and left to equilibrate for 20 min. The pH of the resulting slurry was measured by a calibrated HACH HQ30d pH meter. To measure anions in sediments, 2 g of dry sediment was mixed with 10 mL of distilled water, shaken for 5 min, and left to equilibrate for 4 h. The supernatant was then centrifuged 3500 ×*g* for 15 min and filtered with a 0.45-μm filter membrane. The filtered sample was then used for the determination of anions using ion chromatography (DIONEX ICS-1500, Sunnyvale, USA). Total sulfur, soluble sulfur, TOC, and total inorganic carbon (TIC) in sediments were measured by an elemental analyzer (Elementar, Hanau, Germany) (Schumacher, 2002). The sediment samples were fully digested with HF and HNO_3 (5:1 in *v*/v) (Edgell, 1989) and then the major and trace elements were determined by ICP-OES (Vista MPX, Varian, USA) and ICP-MS (Agilent, 7700×, California, USA), respectively.

2.3. Sequential extraction analysis of metal(loid)s in sediment samples

A three-stage sequential extraction, adapted from the previous procedure for As by Wenzel et al. (2001) and Gault et al. (2003), was performed to target a range of metal(loid)s phases in the sediments. Briefly, 1 g of sediment was placed in a 50 mL centrifugation tube. The "easily exchangeable fraction" was extracted through the addition of 10 mL of 0.05 M $(NH_4)_2SO_4$ solution followed by constant agitation for 4 h. Next, the "specifically-sorbed surface-bound fraction" was extracted by shaking the residual sediment with 10 mL of 0.05 M $NH_4H_2PO_4$ for 16 h. Finally, a fraction containing "amorphous hydrous oxides of iron (and aluminum)" was targeted by the addition of 10 mL of 0.2 M ammonium oxalate buffer (pH 3.0), followed by a 4 h reaction time in the dark. All equipment was acid-washed and all reagents were analytical grade (Kemoiou, Tianjing, China). Extractions were performed at room temperature (~20 °C) in 50 mL centrifugation tubes and all shaking was done at 200 rpm. After each extraction stage, samples were centrifuged at 3000 rpm for 15 min and the supernatant was removed and analyzed by ICP-MS (Agilent, 7700×, California, USA). The detection limits for Sb, calculated as the average of ten times the standard deviation of the ion counts obtained from the individual procedural reagent blanks (prepared in the same way as the sample decomposition), were 0.2 μg/L and 1 mg/kg for water and sediment samples, respectively. The certified reference materials (SLRS-5 (Fornieles et al., 2011; Rueda-Holgado et al., 2012)) and internal standards (Rh at 500 μg/L (Ning et al., 2015)) were used for accuracy testing. The standard reference material GBW07310 (Chinese National Standard) was used for analytical quality control. The measured total Sb concentration in GBW07310 was 6.46 ± 0.8 mg/kg, which is comparable to the certified value of 6.3 ± 0.9 mg/kg.

2.4. Scanning electron microscopy (SEM) and energy-dispersive X-ray spectrometer (EDS)

SEM analysis was used to determine the presence and morphology of minerals in the sediments based on a protocol described previously (McBeth et al., 2013). SEM images were taken on a field-emission scanning electron microscope (JSM-6460LV, JEOL, Tokyo, Japan) with an EDAX energy-dispersive X-ray spectrometer (EDAX-GENESIS, Mahwah, USA). The SEM was operated at 15 kV with a working distance of 10 mm. For X-ray analysis, an accelerating voltage of 20 kV was used to obtain sufficient X-ray counts.

2.5. High-throughput sequencing of the V4 region of 16S rRNA genes

Total genomic DNA was extracted from 10 g of homogenized sediment samples using the FastDNA® spin kit (MP bio, Santa Ana, USA) following the manufacturer's protocol. All DNA extracts were stored at −80 °C until further analysis. DNA concentration and purity was monitored on 1% agarose gels. The V4 region of 16S rRNA genes was amplified using the 515f/806r primer set (Caporaso et al., 2011). 16S rRNA tag-encoded ultra-high-throughput sequencing was carried out on the Illumina MiSeq platform at Novogene (Beijing, China). Sequences were analyzed with the Quantitative Insights Into Microbial Ecology (QIIME) software and UPARSE pipeline (Caporaso et al., 2010). Paired-end reads were merged using FLASH (Magoč and Salzberg, 2011). The merged reads were then assigned to samples based on the barcodes and truncated by cutting off the barcode and primer sequences. The raw reads were filtered using split_libraries_fastq.py in QIIME(V1.7.0) with the following criteria: maximum number of consecutive low quality base calls = 3; minimum number of consecutive high quality base calls as a fraction of the read length = 0.75, no base calls with Phred score <3 (Bokulich et al., 2013; Caporaso et al., 2010). The tags were

then compared with the reference database (Gold database, http://drive5.com/uchime/uchime_download.html) using UCHIME (http://www.drive5.com/usearch/manual/uchime_algo.html) to detect and remove chimera sequences (Haas et al., 2011). UPARSE was used to cluster operational taxonomic units (OTUs) at 97% similarity and the RDP classifier (Version 2.2, http://sourceforge.net/projects/rdp-classifier/) was used to assign taxonomy (DeSantis et al., 2006; Wang et al., 2007) based on the Green Genes Database (http://greengenes.lbl.gov/cgi-bin/nph-index.cgi). Chao1 and Shannon indices were used to estimate species richness for the six libraries (Schloss et al., 2009).The reads were deposited into the NCBI short reads archive database under accession number of SRP056490.

2.6. Data analyses

The similarity of microbial communities among different sediment samples was determined using both weighted and unweighted UniFrac. UPGMA (Unweighted Pair Group Method with Arithmetic mean) clustering was conducted on weighted UniFrac (Kuczynski et al., 2012). The distribution of the dominant phyla was visualized by using Circos software (Krzywinski et al., 2009), and the Circos graphs were produced *via* Circos software online (http://circos.ca/). Canonical correspondence analysis (CCA) performed by CANOCO 4.5 (Microcomputer Power, Ithacha, NY) was used to measure chemical properties that had the most significant influence on microbial community structure. CCA is a robust multivariate method for directly correlating the environmental data with species. CCA was done on abundant bacteria genera (*i.e.*, relative abundance >1% in at least one sequencing library) and selective environmental parameters. A symbol's position in relation to a vector head indicates the correlation between the community and the environmental factors. The length of a vector reflects the relative importance of those environmental factors in discriminating the overall microbial community within one library (Zhang et al., 2008). Manual forward selection with Monte Carlo permutation tests was then performed to determine the significance of the environmental variables with 999 permutations (Lepš and Šmilauer, 2003). CCA was performed focusing on interspecies difference. The CCA bipolar were generated by CanoDraw 4.0 (Microcomputer Power, Ithacha, NY). Two CCA were performed in the current study: one to correlate water geochemical data with species and one to correlate sediment geochemical data with species. The correlations between geochemical parameters and the relative abundances of different phyla or genera were determined by Spearman's rank correlation using SPSS (v19) package. Unless stated, p values <0.05 were considered significant. Spearman's rank correlation coefficient is a nonparametric method to evaluate the relationship between two independent variables without normality assumption of the raw data (Corder and Foreman, 2014). Only microbial genera that represented >1% of the total community in at least one sequencing and the major geochemical parameters of interest (Sb and As fractions, metal(loid)s showing high concentrations, parameters showing significant correlations by CCA) were selected for this analysis.

3. Results

3.1. Analysis of the environmental data set

The physicochemical characteristics of the water samples were determined at six sampling sites as shown in Tables 1 and S1. The pH of water samples ranged from 6.97 at EW to 10.82 at CW (Table 1). Aqueous sulfate concentrations were relatively higher in Dajiagou River, ranging from 135 to 427 mg/L, compared to 95 to 208 mg/L in Chahe River (Table 1). Redox potential (Eh) varied between 62.5 and 99.4 mV in Dajiagou River and decreased to −3.6 to −23.6 mV in the Chahe River, located downstream. The highest TOC concentration was found at the most upstream sampling site (AW, 24.9 mg/L) and decreased downstream. Aqueous nitrate concentrations were relatively constant in the watershed, ranging from 4.02 (BW) to 7.05 mg/L (CW).

Geochemical parameters for the sediment samples are shown in Tables 2 and S2. Total Fe in the sediment ranged from 14.9 (FS) to 33.7 g/kg (ES). All sediment samples showed pH values greater than 7 with the exception of BS (pH = 3.02). The maximum sulfate concentration occurred at sample location CS with a value of 2084 mg/L. Sulfate concentrations gradually decreased downstream with a minimum concentration of 474 mg/L at ES. Other geochemical parameters such as TOC, total S, nitrate, total N, and total C were also determined, as shown in Table 2. Like TOC in the water, the highest TOC concentration was found at AS but decreased downstream. Sulfate concentrations were relatively higher in upstream sites while sulfate concentrations decreased in downstream samples.

3.2. Sb and As fractions in water and sediments

Aqueous Sb concentrations (Sb_{aq}) in all samples were at least 29 times greater than the maximum contaminant level goal (MCLG) and maximum contaminant level (MCL) of 6 μg/L, as established by the USEPA (1979). Specifically, Sb_{aq} ranged from 172 (FW) to 3248 μg/L (AW) (Table 3). Sb_{aq} decreased in Chahe River due to dilution with uncontaminated water from tributaries. In comparison, total Sb concentrations in the sediments (Sb_{sed}) ranged from 1849 to 16,071 mg/kg. The highest Sb concentration was detected in the sediment from Chahe River (ES), followed by one sample (DS) in Dajiagou River. The lowest Sb_{sed} concentration was also detected from a site in the Chahe River (FS), located downstream of the ore dressing plant, with a concentration of 1849 mg/kg.

Sequential extractions were used to infer specific Sb association with the aim of providing useful information on potential metalloid mobility and bioavailability in the sediments. The fractionation of Sb and other targeted metal(loid)s (Tables 3, S3–S5) were measured in sediment samples. Sequential extractions demonstrated that the exchangeable Sb fractions (Sb_{exc}) varied between 0.003% (ratio of Sb fractions to Sb_{sed}, hereafter) (AS) and 1.7% (FS). Specifically-sorbed surface-bound Sb fractions (Sb_{srp}) ranged between 0.3% (BS) and 8.7% (CS). Sb_{amr}, which represents the poorly mobilizable and bioaccessible Sb fraction (Buanuam and Wennrich, 2010; Savonina et al., 2012), demonstrated higher concentrations in AS-CS (11% to 15%), but decreased in DS and

Table 1
Chemical and physical parameters of the river water samples (sampled at the surface) from each site.

Sample	pH	T (°C)	Eh (mV)	Con (μS/cm)	TDS (mg/L)	Sal (‰)	TOC (mg/L)	F^- (mg/L)	Cl^- (mg/L)	NO_3^- (mg/L)	SO_4^{2-} (mg/L)
AW	9.7	11.5	80.8	577	380	0.38	24.9	1.0 ± 0.4	2.03 ± 0.04	6.73 ± 0.29	427 ± 16
BW	9.23	11.9	93.4	399	254	0.25	5.2	0.43 ± 0.12	2.43 ± 0.06	4.02 ± 1	262 ± 14.7
CW	10.82	11.4	62.5	349	226	0.23	4.4	0.27 ± 0.07	2.4 ± 1.4	7.05 ± 0.68	135 ± 58
DW	8.95	10.8	99.4	396	259	0.26	2.9	0.26 ± 0.02	2.01 ± 0.09	4.38 ± 0.26	247 ± 5.8
EW	6.97	19.6	−23.6	455	241	0.24	1.5	0.26 ± 0.02	5.16 ± 0.12	5.1 ± 1.22	208 ± 5.3
FW	8.1	19.5	−3.6	219	172.3	0.17	3.6	0.1 ± 0.02	7.56 ± 0.56	4.71 ± 1.81	95 ± 8.2

Abbreviation: T, temperature; Con, conductivity; TDS, total dissolved solids; Sal, salinity.

Table 2
Physicochemical parameters of the river sediments from each site.

Sample	pH	Total Fe (g/kg)	Total N(%)	Total C(%)	TOC (%)	Cl^- (mg/kg)	NO_3^- (mg/kg)	SO_4^{2-} (mg/kg)
AS	10.16	28.3 ± 1.7	0.06 ± 0.01	4.3 ± 0.9	0.2 ± 0.07	2.8 ± 0.02	3.4 ± 2.3	1449 ± 10
BS	3.02	29 ± 0.2	0.15 ± 0.005	0.8 ± 0.01	0.5 ± 0.16	3.8 ± 0.47	4.9 ± 1.2	1122 ± 30
CS	7.21	16.7 ± 0.2	0.10 ± 0.001	0.9 ± 0.1	0.7 ± 0.02	2.1 ± 0.9	0.7 ± 0.3	2084 ± 124
DS	7.41	22.8 ± 0.4	0.07 ± 0.002	0.6 ± 0.3	0.1 ± 0.001	3.7 ± 1.05	<0.01	683 ± 114
ES	7.73	33.7 ± 0.2	0.05 ± 0.005	0.8 ± 0.1	0.1 ± 0.001	1.3 ± 0.02	3.3 ± 1.6	474 ± 14
FS	7.69	14.9 ± 0.3	0.06 ± 0.006	0.7 ± 0.1	0.1 ± 0.004	2.1 ± 0.07	4.0 ± 2.0	900 ± 28

FS (0.3% to 3%). For the poorly bioaccessible Sb fractions, only amorphous Fe and Al oxide-bonding Sb (Sb_{amr}) was measured. Other metal(-loid)s such as Zn, As, and Ba demonstrated higher concentrations than other tested metal(loid)s (Tables S3–S5). SEM-EDS analyses showed that Sb was one of the major components in the mineralized structures of sediments (Fig. 2). Interestingly, the presence of Sb peaks was collocated with S and O peaks, suggesting that potential Sb minerals may have been the Sb bearing sulfides and/or oxides such as stibnite (Sb_2S_3) and valentinite (Sb_2O_3). However, Sb was not evenly distributed in the sediment particles: semi-quantitative analysis of the SEM-EDS showed that some particles with high Sb content were adjacent to the ones exhibiting low Sb or even no Sb peaks (Fig. S1).

3.3. General analyses of the Illumina-derived dataset

In total, approximately 403,938 raw sequence reads of the 16S rRNA gene spanning the hyper variable V4 region were obtained from the six sediment samples. After filtering the low quality reads and chimeras, a total of 336,003 valid reads (average read length 255 bp) were used for subsequent downstream analyses. The numbers of tags for phylogenetic analysis and OTUs (97% similarity) were summarized in Fig. S2 and Table 4. The library derived from sampling site ES had the greatest number of OTUs (3641) while that from FS had the least number of OTUs (1458). It is notable that a large number of reads (23.4% of total reads) only occurred once across all samples (Fig. S2).

3.4. Taxonomic profile

Altogether, more than 40 phyla were recovered from the six sediment samples. The weighted UPGMA tree showed that microbial communities in Dajiagou River more closely resembled each other than those taken from Chahe River (Fig. 3). The general taxonomic pattern was mainly driven by differences in the abundances of major taxonomic groups. The majority of these reads were affiliated with known members of *Proteobacteria*. This phylum accounted for 60.8% of total reads (35.9% to 83.3% in the six libraries) and was more abundant in Chahe River than Dajiagou River (Fig. 4). *Firmicutes* was the second most abundant phylum (9% of total reads), accounting for 4.2%–29.3% of total valid reads in each sample. Other major phyla included *Bacteroidetes* (3.5%–16.5%), *Actinobacteria* (2.2%–11%), *Acidobacteria* (1.4%–5.5%), and *Cyanobacteria* (0.5%–4.3%). Within *Proteobacteria*, *Betaproteobacteria* was the most abundant class, accounting for 27.2% of total reads, followed by *Gammaproteobacteria* (17.5%), *Alphaproteobacteria* (7.5%), and *Deltaproteobacteria* (5.9%). *Betaproteobacteria* constituted a substantial portion of the library for FS but was less abundant in libraries of AS and DS. *Gammaproteobacteria* had greater abundance in the libraries derived from Dajiagou River (BS and CS) but was less abundant in that of FS. Other classes that occurred in all the sediment samples included *Clostridia*, *Bacilli*, *Bacteroidia*, *Actinobacteria*, *Sphingobacteriia*, and *Flavobacteriia* (Table 5). As indicated by a previous study, the 515f/806r primer pair is nearly universal to archaea and bacteria (Walters et al., 2011). In accordance with this, archaeal phyla were also detected in all samples (Fig. S3), accounting for 1.3% of total valid reads. The archaeal phyla detected were *Crenarchaeota* (91.3% of all archaeal reads) and *Euryarchaeota*. At the genus level, the microbial composition differed substantially in the six sequencing libraries. Some genera showed relatively high abundances in sequencing libraries derived from Dajiagou River while some genera demonstrated higher reads in libraries derived from Chahe River. Therefore, a graph of abundance of various microbial groups in both Chahe and Dajiagou Rivers was constructed to visualize this difference (Fig. 5). As illustrated from this graph, *Acidovorax*, *Sulfuricurvum*, *Flavobacterium*, *Geobacter*, *Thiobacillus*, *Dechloromonas*, *Rhodobacter*, and *Hydrogenophaga* were more abundant in the sequencing libraries from sediments of Chahe River. In contrast, *Shewanella*, *Lactobacillus*, *Clostridium*, and *Acinetobacter* occurred at high levels in libraries derived from sediments of Dajiagou River. Detailed information about the relative abundances of dominant genera in each sample is provided in the heat map (Fig. S4).

3.5. Relationship between microbial community and the environment

Canonical correspondence analysis (CCA) was performed to discern possible linkages between the microbial communities and geochemical parameters from either water (Fig. 6(a)) or sediments (Fig. 6(b)). In Fig. 6(a), CCA axis 1 was positively correlated with water temperature, but was negatively correlated with aqueous sulfate, Eh, pH, Sb and TOC. The relatively low magnitude of Mn, As, and nitrate vectors indicated that these aqueous factors were not as strongly correlated to community composition as other tested factors. In Fig. 6(b), CCA axis 1 was positively correlated with total Fe and nitrate in sediments, but was negatively correlated with pH. Sulfate, Mn, and TOC in sediments were also strongly linked to bacterial community variance. In addition, Sb_{exc} and Sb_{amr} were significantly linked to microbial community compared to Sb_{srp} and Sb_{sed}.

To test the interaction between community members and Sb contamination, Spearman's rank correlation was used to compare the correlation between bacterial taxa (phyla and genera) and different Sb fractions as well as other geochemical parameters. As indicated by Spearman's rank correlation, many microbial taxa (phyla and genera) that were abundant (relative abundance >1% in at least one sample)

Table 3
Aqueous Sb concentrations (μg/L) and different Sb extraction fractions (mg/kg) in six sampling sites.

Operationally defined phase	AS (mg/kg)	BS (mg/kg)	CS (mg/kg)	DS (mg/kg)	ES (mg/kg)	FS (mg/kg)
Total digest (Sb_{sed})	3945 ± 196.9	4561	2148 ± 30.4	9751 ± 204.2	16,071 ± 454.7	1849 ± 117.5
Easily exchangeable (Sb_{exc})	0.11 ± 0.02	3.6 ± 0.04	23.9 ± 1.97	10.2 ± 0.28	29.9 ± 1.71	31.2 ± 0.55
Specifically sorbed (Sb_{srp})	18.1 ± 0.52	12.2 ± 0.39	187.2 ± 18.7	28.2 ± 1.45	46.5 ± 2.09	49.2 ± 2.33
Amorphous crystalline hydrous oxides of Fe and Al (Sb_{amr})	440 ± 20.5	577.9 ± 18.3	322.8 ± 15.1	44.9 ± 2.80	53.7 ± 4.56	54.8 ± 0.29
	AW (μg/L)	BW (μg/L)	CW (μg/L)	DW (μg/L)	EW (μg/L)	FW (μg/L)
Aqueous (Sb_{aq})	3248 ± 11.8	2512 ± 5.0	3051 ± 31.9	2689 ± 37.2	1144 ± 10.4	172 ± 0.5

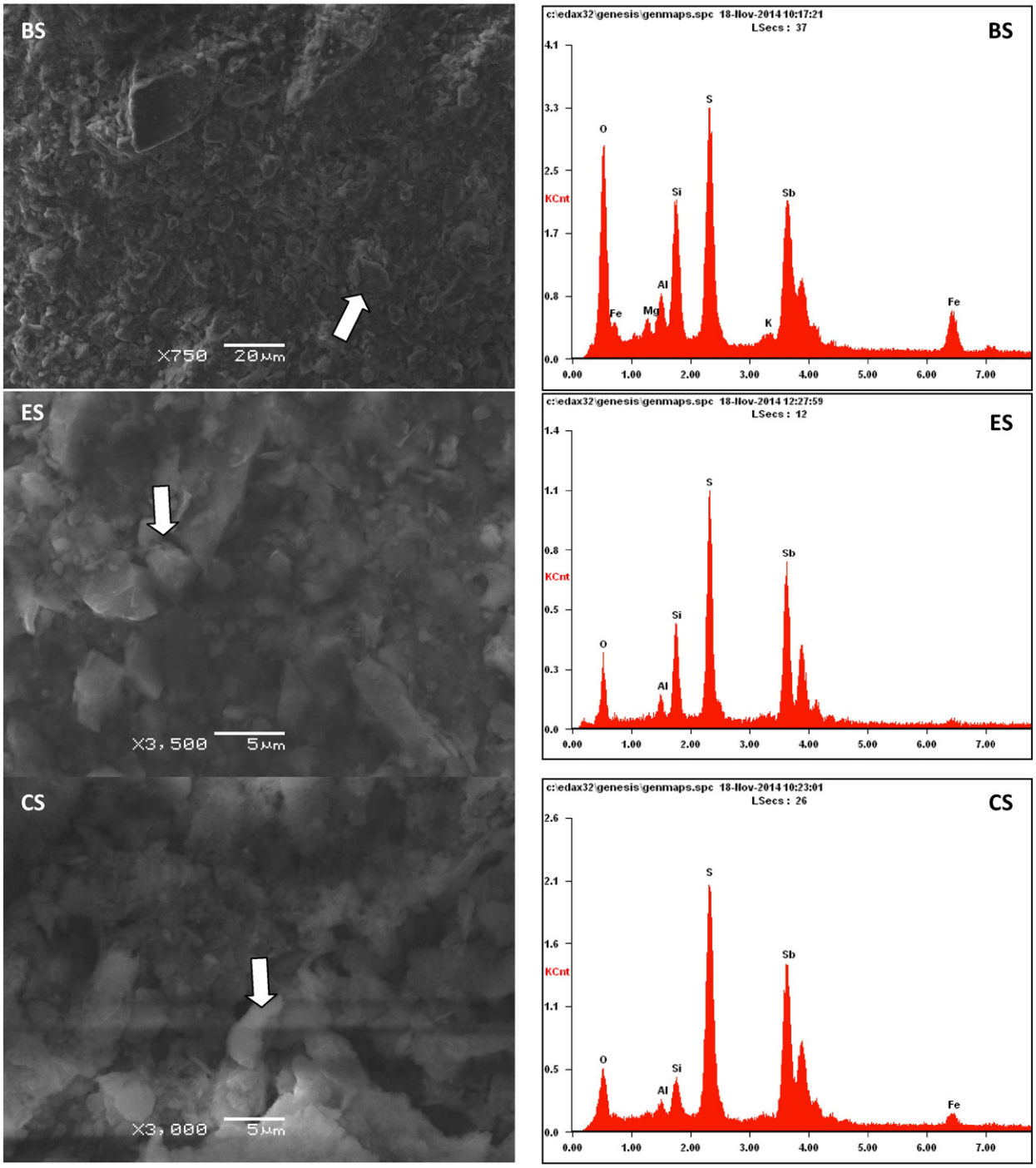

Fig. 2. Representative SEM images (left panel) and the corresponding EDS spectra (right panel) of the sediment samples. Sampling sites were labeled on the top of each figure.

Table 4
Summary of sequencing parameters of six Illumina sequencing libraries.

Sample sites	No. of raw reads	No. of qualified reads	No. of no chimera reads	Average length (bp)	Chao1[a]	Shannon[a]
AS	61,683	51,933	50,587	253	2842.51	9.393
BS	104,514	104,042	103,288	253	2888.64	8.274
CS	40,103	37,496	36,917	253	2233.47	8.745
DS	62,083	55,288	54,157	255	2828.12	9.73
ES	135,555	134,995	134,088	255	3454.9	8.118
FS	100,046	99,051	97,952	257	1495.06	7.237

[a] OTU were defined at 97% sequence similarity.

had significant correlations ($p < 0.05$, hereafter) with different Sb fractions (Fig. 7). At the phylum level, Sb_{exc} was positively correlated with *Betaproteobacteria* ($r = 0.829$) while Sb_{sed} was positively correlated with *Cyanobacteria* ($r = 0.829$). At the genus level, *Acinetobacter* ($r = 0.943$), *Sphingomonas* ($r = 0.943$), *Geobacter* ($r = 0.928$), and *Kaistobacter* ($r = 0.829$) had positive correlations with Sb_{aq} while *Sulfuricurvum* ($r = -0.928$) was negatively correlated with Sb_{aq}. In addition, Sb_{sed} had a positive correlation with *Staphylococcus* ($r = 0.829$) and *Rhodoplanes* ($r = 0.812$). Sb_{exc} was positively correlated with *Rhodoferax* ($r = 0.829$), *Acidovorax* ($r = 0.829$), and *Hydrogenophaga* ($r = 0.899$) but was negatively correlated with *Escherichia* ($r = -0.829$), *Nitrosopumilus* ($r = -0.943$), and *Streptophyta*

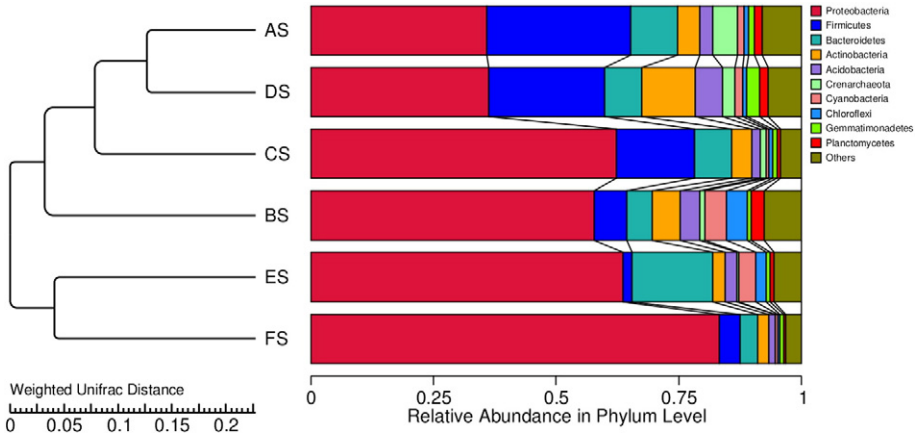

Fig. 3. The UPGMA tree showing clusters of microbial communities based on weighted UniFrac with 100% support at all node.

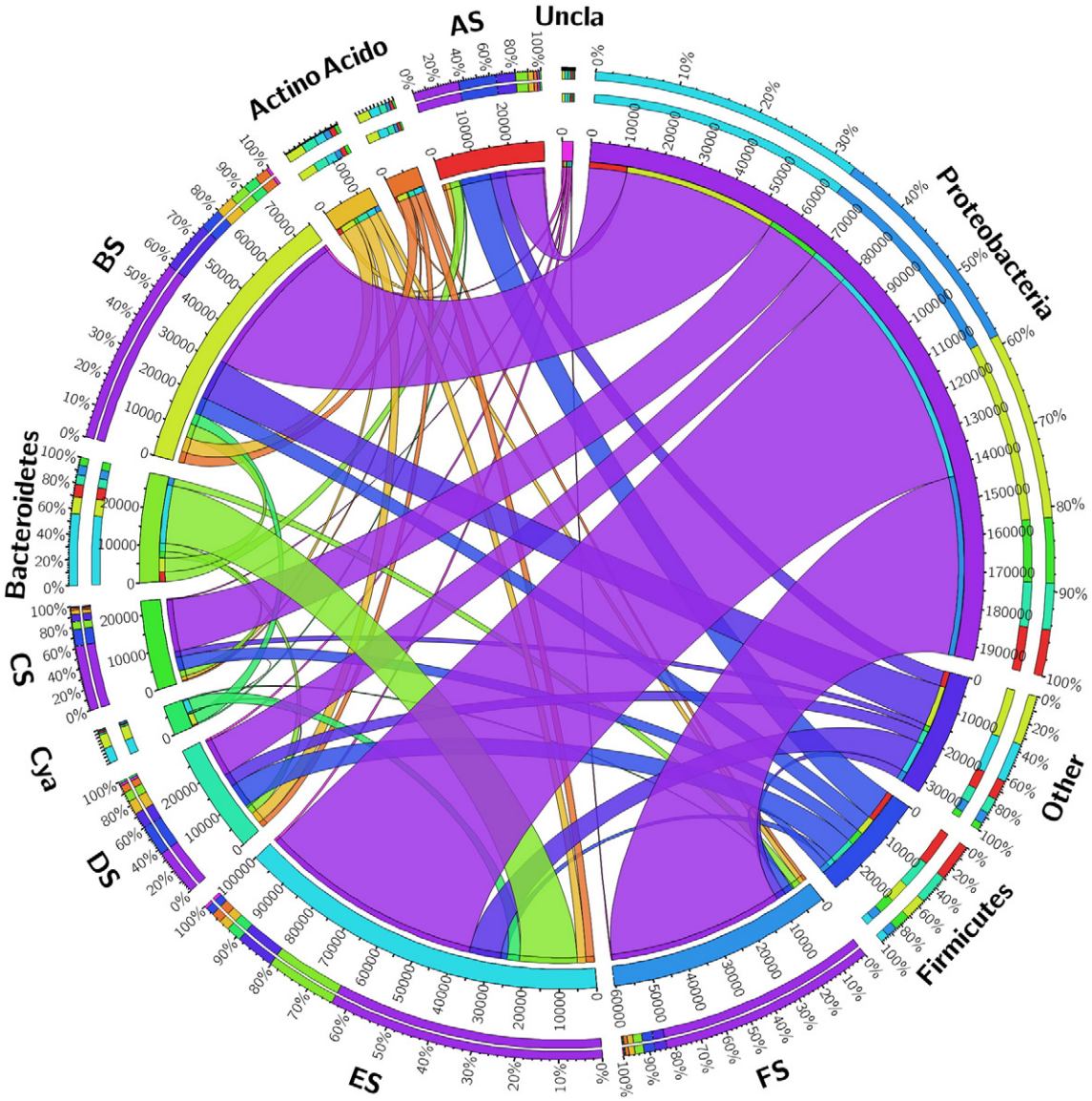

Fig. 4. Distributions of dominant phyla in total sequences in the 6 sediment samples. The data were visualized *via* Circos software (http://circos.ca/). The length of the bars on the outer ring and the number on the inner ring represent the percentage of the phyla to total effective reads and the amount of reads of the corresponding phyla in each sample, respectively. The bands with different colors demonstrate the source of different phyla. Abbreviation: Actino, *Actinobacteria*; Acido, *Acidobacteria*; Cya, *Cyanobacteria*; and Uncla, Unclassified.

Table 5
Microbial community composition as shown as relative abundance in the Chahe watershed at class level.

Taxonomy	AS	BS	CS	DS	ES	FS
Gammaproteobacteria	18.1	30.1	26.6	15.7	11.4	9.0
Clostridia	18.0	1.4	11.4	16.4	1.1	1.6
Betaproteobacteria	9.3	10.7	25.2	9.0	34.0	54.8
Bacilli	8.6	5.1	2.8	4.7	0.7	2.1
Bacteroidia	7.4	1.8	4.1	3.9	4.8	0.4
Alphaproteobacteria	5.4	10.0	8.7	9.1	5.9	7.1
Thaumarchaeota	5.0	0.8	1.2	2.6	0.3	0.0
Deltaproteobacteria	2.7	6.1	1.6	2.2	8.0	7.4
Actinobacteria	2.1	4.8	2.1	3.9	1.8	1.5
Fusobacteria	2.1	0.0	0.4	0.8	0.0	0.0
Sphingobacteriia	1.6	1.9	3.1	2.6	2.8	1.8
Acidimicrobiia	1.5	0.5	1.3	2.9	0.5	0.7
Chloroplast	1.1	3.8	0.5	1.5	1.2	0.5
Planctomycetia	1.0	1.8	0.5	1.3	0.5	0.2
Verrucomicrobiae	0.8	0.1	0.6	0.3	0.0	0.1
Anaerolineae	0.6	3.2	0.5	0.5	1.6	0.2
Chloracidobacteria	0.5	0.4	0.3	1.5	0.2	0.0
Flavobacteriia	0.5	1.2	0.4	0.8	8.5	0.9
Nitrospira	0.4	2.0	0.4	0.4	1.7	0.3
Epsilonproteobacteria	0.3	0.6	0.2	0.2	4.2	4.9
Nitriliruptoria	0.3	0.0	0.3	1.9	0.0	0.0
Oscillatoriophycideae	0.0	0.3	0.0	0.0	2.1	0.0
Deltaproteobacteria	2.7	6.1	1.6	2.2	8.0	7.4

($r = -0.812$). Sb_{srp} was positively correlated with *Comamonas* ($r = 0.812$) and *Rhodobacter* ($r = 0.886$), but was negatively correlated with *Streptophyta* ($r = -0.843$). Sb_{amr} was only positively correlated with *Halomonas* ($r = 0.886$). Various As fractions were also significantly correlated with bacterial taxa. Detailed information is presented in Table S6. Other environmental variables had a statistically significant effect on microbial populations as well. For instance, Eh had a negative correlation with *Rhodoferax* ($r = -0.886$), *Hydrogenophaga* ($r = -0.841$), and *Gallionella* ($r = -0.886$) but was positively correlated with *Streptophyta* ($r = 0.843$). Detailed information of the Spearman's rank correlation is presented in Table S7 (phylum level) and S8 (genus level).

4. Discussion

The elevated Sb concentrations in water and sediments make Chahe watershed a good object to study microbial responses to high Sb environments. Total concentrations of Sb in Chahe sediments were remarkably higher than the background concentration of Sb in China's soils (0.8–3.00 mg/kg) (He et al., 2012). Among all six sediment samples, ES displayed the highest Sb_{sed} concentration (16,071 mg/kg), possibly due to the reception of Sb-rich sludge from the ore dressing plant and the mining activities along the Dajiagou River. Typical aqueous Sb concentrations in unpolluted water are less than 1 μg/L according to the survey of water geochemistry worldwide (Filella et al., 2002). However, due to mining activities, Sb_{aq} reached up to 3250 times the natural concentration and was 540 times greater than the MCLG set by USEPA. Specifically, Sb_{aq} was higher in Dajiagou River but decreased in Chahe River mainly due to dilution by uncontaminated tributaries.

In general, the mobility, bioaccessibility, and potential toxicity of metals and metalloids in sediments were strongly correlated with the forms in which they occur and the type of binding with the sample matrix (Savonina et al., 2012). The co-occurrence of Sb, as well as S and/or O peaks in SEM–EDS analysis, indicated that Sb may be present in the form of sulfides and oxides in the sediment, suggesting existence of minerals such as stibnite (Sb_2S_3), valentinite (Sb_2O_3), and cervantite (Sb_2O_4), all of which have commonly been found in the earth's crust (Wilson et al., 2010). Sequential chemical extractions were employed to infer metal(loid)s association with specific phases such as minerals or organic compounds. Among these sequential extractions, Sb_{exc} and Sb_{srp} were considered as bioaccessible Sb fractions while amorphous Fe and Al oxide-bound Sb (Sb_{amr}) and crystalline Fe and Al oxide-bonding Sb (not measured in this study) were considered as poorly bioaccessible fractions (Buanuam and Wennrich, 2010; Savonina et al., 2012). Exchangeable or weakly bound Sb typically constituted only a small proportion of the total soil concentration (Wilson et al., 2010) and in the current study, the Sb_{exc} and Sb_{srp} fractions constituted only 0.5%–10.96% of total Sb_{sed}. This suggests that the mobility and bioaccessibility of Sb is low in Chahe watershed despite the elevated total Sb concentrations, which is in accordance with previous studies (Filella et al., 2002). The Sb_{exc} and Sb_{srp} accounted for higher proportion in downstream samples compared to upstream samples (AS and BS).

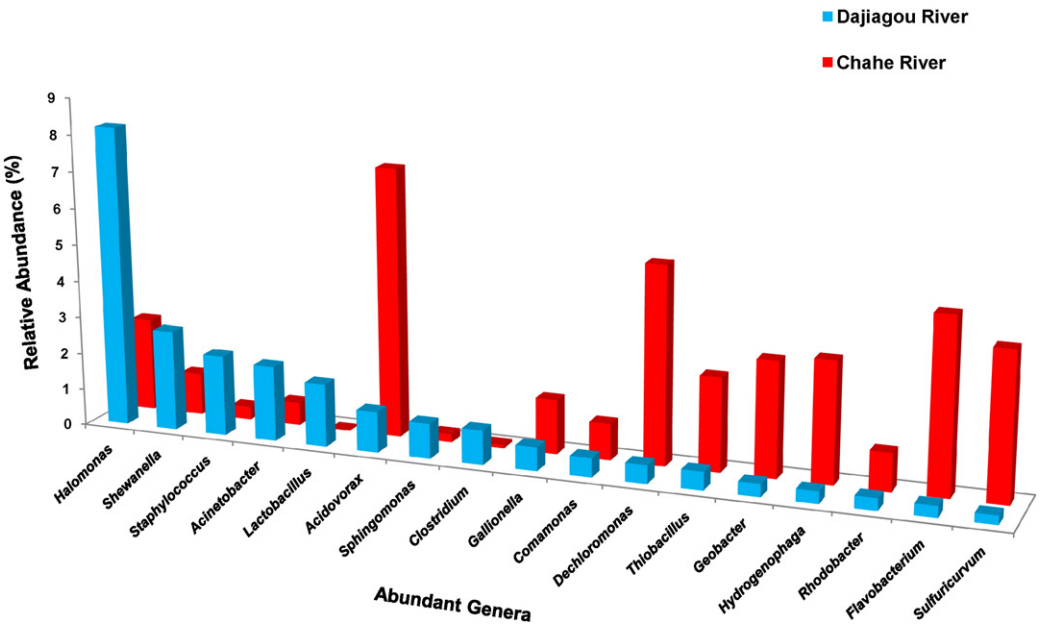

Fig. 5. Profile visualizing the 17 most abundant genera among six sequencing libraries derived from sediment samples. Sequencing libraries were divided into two groups based on which river they were taken from. These figures represented the relative abundances of a genus in the group from Dajiagou River or Chahe River.

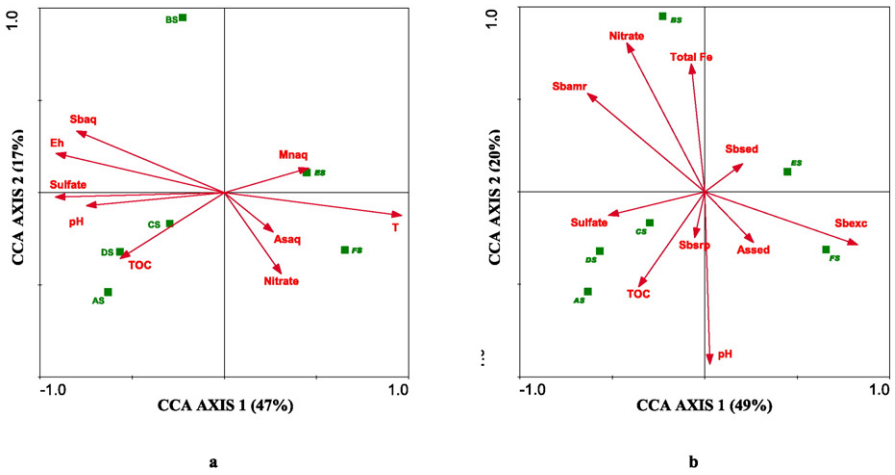

Fig. 6. Canonical correspondence analysis (CCA) of 16S rRNA gene data and geochemical parameters from water (a) and sediments (b). Arrows indicate the direction and magnitude of geochemical parameters associated with bacterial community structures. Abbreviations: T(temperature); Sbaq (aqueous Sb); Asaq (aqueous As); Assed (total As in sediment); Sbsed (total Sb in sediment); Sbexc (easily exchangeable Sb species); Sbsrp (specifically sorbed forms of Sb); Sbamr (amorphous hydrous oxides of Fe and Al); and Total Fe (total concentration of Fe in sediments).

This may be due to the fact that Sb is oxidized along the Dajiagou River and finally precipitated in downstream sediment. These oxidized forms of Sb may be more bioaccessible than mineral-bound Sb (Johnson et al., 2005). The co-occurrence of Sb and Fe peaks (Figs. 2 and S1) indicated a potential adsorption of Sb by Fe oxyhydroxides, which is confirmed by the detection of Sb_{amr} along the watershed. Fe oxyhydroxides are major carrier phases for Sb and such adsorption is a common phenomenon as reported previously (Ashley et al., 2003).

Although a large portion of the Sb was associated with immobile Sb fractions, the geochemical parameters still affected the overall microbial communities as well as the individual bacterial taxa according to the results of CCA and Spearman's rank correlation. Specifically, CCA indicated a considerable relationship between the microbial community structure and three Sb fractions, Sb_{aq}, Sb_{exc}, and Sb_{amr} (Fig. 6), indicating these Sb fractions may act as stressors to influence the composition and diversity of sediment microbial community. Since both the Dajiagou and Chahe Rivers have only shallow (~3 cm) sediment layers on top of the rocky river bed, only surface sediment samples were collected. Due to this shallow sediment layer, Sb_{aq} may be easily accessible by microorganisms and thus, have an impact on overall microbial communities. Sb_{exc} is considered easily mobilizable and bioaccessible and thus may influence the overall microbial communities (Savonina et al., 2012). However, Sb_{amr} is much less mobilizable and accessible to microorganisms (Savonina et al., 2012). This correlation may require further investigations. In

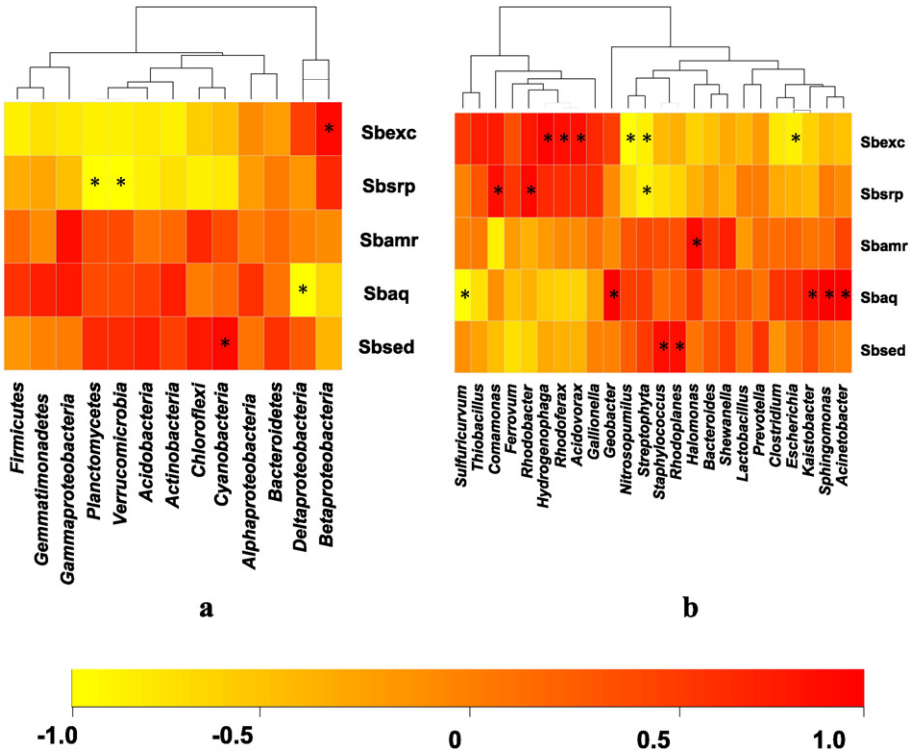

Fig. 7. Heat maps of Spearman's rank correlations coefficients and cluster analysis between the different Sb forms and the relative abundance of bacterial phylum with relative abundances >5% in at least one sample (a) or genera with relative abundances >1% in at least one sample (b). The correlation coefficients are indicated by hue. *, significant correlations (at $p < 0.05$). Abbreviations: Sbexc (easily exchangeable forms of Sb); Sbsrp (specifically sorbed forms of Sb); Sbamr (amorphous hydrous oxides of Fe and Al); Sbaq (aqueous Sb); and Sbsed (total Sb in the sediments).

contrast, the relatively small magnitude of the Sb_{sed} and Sb_{srp} vectors (Fig. 6(b)) indicate these two Sb fractions were not as strongly correlated with community composition as Sb_{aq}, Sb_{exc}, or Sb_{amr}. Based on the measurements, Sb_{sed} primarily consisted of poorly bioaccessible Sb fractions (>70%), which may not significantly affect microbial composition.

Other geochemical parameters exhibited strong correlations with overall community composition. pH along the Chahe watershed was mostly greater than 7, and in particular, pH in Dajiagou River was higher than Chahe River. CCA identified both pH in the water and sediment as a major environmental factor in affecting microbial communities. The pH gradient might exert as a direct selecting pressure by enriching the acidophiles, neutrophiles, or alkaliphiles according to the pH along the watershed. However, more likely, the pH gradient in Chahe watershed may affect the mobility of Sb and other metal(loid)s (Nakamaru et al., 2006). This pH-dependent mobility may affect the adsorption of major metalloids (*i.e.* Sb and As) on minerals and bacterial cells and thus shape the innate microbial communities (Pokrovsky et al., 2014). Meanwhile, redox potential (Eh) is also recognized as an important parameter for structuring the community structure and changed dramatically along the watershed. It is noteworthy that metalloid oxidation state and mobility are mainly determined by system Eh (Sadiq, 1997). The solubility of Sb was correlated with the redox potentials as oxidizing conditions favor higher Sb solubility while lower Sb solubility was found in reducing conditions (Ashley et al., 2003). Therefore, the variation of these factors may result in difference in metalloid oxidation state and bioaccessibility, consequently driving changes in composition and diversity of sediment microbial community. Aqueous nitrate and sulfate concentrations, TOC, and water temperatures were also substantially correlated with the microbial communities, indicating that the overall microbial communities were shaped by a suite of geochemical variables.

The significant changes of several geochemical parameters such as Sb_{aq} and Sb_{amr} in the Dajiagou and Chahe River create pollution gradients, which in turn structure the microbial composition and diversity. Therefore, Spearman's rank correlation was used to evaluate the correlation between abundant taxonomic groups and geochemical parameters. In general, excessive concentrations of heavy metal(loid)s can be toxic to microorganisms and disrupt their growth. In this study, however, many bacterial phylotypes were positively correlated with different Sb fractions, suggesting that the elevated Sb did not inhibit them as much as other microbial taxa. Another remarkable finding was that many genera positively correlated with different Sb fractions have been reported previously as As-metabolizing bacteria such as *Geobacter* (Giloteaux et al., 2012) and *Sphingomonas* (Kinegam et al., 2008). This suggests that organisms may exhibit similar physiological traits in response to the contaminants with similar chemical properties.

Some genera which contain species that are able to metabolize or resist Sb were positively correlated with different Sb fractions. Among these genera, *Acinetobacter* contains some species, such as *Acinetobacter* sp. JL7 (Li et al., 2013), which are able to oxidize Sb(III) (Li et al., 2013; Shi et al., 2013) while *Sphingomonas* spp. are known for their ability to reduce As(V) or oxidize As(III) (Kinegam et al., 2008; Macur et al., 2004). Given the broad similarities between As and Sb, it was hypothesized that *Sphingomonas* and *Acinetobacter* may be able to carry out Sb reactions. Recently, Shi et al. isolated *Sphingopyxis*-like isolates that were able to oxidize Sb(III) (Shi et al., 2013) from different mining soils (both *Sphingomonas* and *Sphingopyxis* are in the family *Sphingomonadaceae*.). In addition, 16S rRNA genes closely related to *Sphingomonas* were detected in high abundances in a Sb- and As-rich mine drainage tailings in Slovakia (Majzlan et al., 2011). Sequences assigned to *Flavobacterium* were highly enriched in Chahe River, especially in ES (7.4%). Jenkins et al. found that pure cultures of *Flavobacterium* sp. were able to biomethylate Sb(III) (Jenkins et al., 2002). In addition, bacteria affiliated with *Flavobacterium* were isolated from As-contaminated soils in Thailand and identified as As-oxidizing bacteria (Kinegam et al., 2008), indicating a linkage of this genus with the Sb–As-rich environments. Sb_{sed} was positively correlated with *Staphylococcus*, a genus containing several species with resistance to heavy metals, including Sb and As (Corbisier et al., 1993; Endo and Silver, 1995). For example, plasmids in *Staphylococcus aureus* contain an "operon" that provides resistance to As(III), As(V), and Sb(III) salts (Silver et al., 1981), while *Staphylococcus xylosus* contains plasmid pSX267 that similarly contains an As(III), As(V), and Sb(III) resistance region (Kreutz and Götz, 1984). This resistance to Sb may explain the positive correlation between *Staphylococcus* and Sb_{sed}.

Genera containing species that participate in As cycling were also found to be positively correlated with various Sb fractions. Both *Acidovorax* and *Hydrogenophaga* are positively correlated with Sb_{exc} and contain As-oxidizing species (Huang et al., 2012; vanden Hoven and Santini, 2004). The genus *Acidovorax*, which contains both As(III)-oxidizing (Huang et al., 2012) and As(V)-reducing species (Lear et al., 2007), was highly enriched in ES (7%) and FS (7.9%). Like *Acidovorax*, *Hydrogenophaga* spp. were detected in high numbers in Chahe River (ES (1.9%), FS (5.6%)). *Hydrogenophaga* contains As(III)-oxidizing strains such as *Hydrogenophaga* sp. str. NT-14 (vanden Hoven and Santini, 2004). *Hydrogenophaga* was also detected in As-rich deltaic aquifers and identified as the major As-oxidizing bacterial genus (Ghosh et al., 2014). *Halomonas* was positively correlated with Sb_{amr} and was highly enriched along the watershed. *Halomonas* contains strains that are able to oxidize As(III) (Hamamura et al., 2014; Lin et al., 2012). In a recent study, a *Halomonas* strain from an alkaline saline lake in Khovsgol, Mongolia was found to contain a novel arsenite oxidase (Hamamura et al., 2014).Although direct evidence of Sb respiration was not found in these bacteria, the involvement of these bacterial genera in As metabolism indicates that they may play an ecological role in Sb cycling. These potential Sb- and As-oxidizing bacteria hold the likelihood to oxidize more toxic Sb(III) to less toxic Sb(V) (Wilson et al., 2010), which would be beneficial to the clean-up of Sb-contaminated sites.

Shewanella, *Rhodoferax*, and *Geobacter*, enriched along the watershed, are Fe(III)-reducing bacteria (FeRB) and may play a major role in the mobilization of Sb and As, which may subsequently be reduced by As- and Sb-reducing bacteria. However, we could not exclude the possibility of these FeRB in reduction of Sb. Many FeRB are capable of respiring using other metal(loid)s as electron acceptors(Liu et al., 2002; Lovley et al., 1993). For example, *Shewanella* was able to reduce Fe, Mn, and As under different redox conditions (Fredrickson et al., 2002; Heidelberg et al., 2002; Saltikov et al., 2005). *Geobacter*, which is positively correlated with Sb_{aq}, is also well known for its ability to reduce metals (Lovley et al., 1993, 2004). Giloteaux et al. found that *arrA*, which encodes for the dissimilatory As(V) reductase, and *acr3*, which encodes for the arsenic pump protein Acr3, were most similar to *Geobacter lovleyi* and *Geobacter uraniireducens*, indicating *Geobacter* species may play a significant role in As biogeochemistry (Giloteaux et al., 2012). In this study, *Geobacter* demonstrated high relative abundances in sediments with elevated Sb contents, suggesting *Geobacter* may also tolerate or metabolize Sb as they do on As compounds. The genus *Rhodoferax*, which is positively correlated with Sb_{exc}, contains some dissimilatory Fe(III)-reducing species (Finneran et al., 2003). In addition to being FeRB, the genome of *Rhodoferax ferrireducens* contains a cluster of genes related to As metabolism (Risso et al., 2009). These results collectively suggest a possible role of these FeRB in Sb(V) reduction.

A number of sulfate reducing bacteria (SRB) were detected along the watershed. Among them, *Clostridium* demonstrated higher abundance in Dajiagou River, which is in consistent with the observation of greater concentrations of sulfate. *Clostridium collagenovorans* has been shown to biomethylate Sb in anaerobic digestion of sewage sludge (Michalke et al., 2000). Sulfate reduction could generate sulfide as a reaction product to precipitate heavy metals, including Sb (Johnson and Hallberg, 2005). Wang et al. reported the removal of Sb(V) from Sb mine waters by SRB. They found that sulfides resulting from biological sulfate reduction were able to reduce Sb(V) to Sb(III) and to form Sb_2S_3 (Wang et al., 2013). Thus, SRB may have the potential for site remediation in the

contaminated sites with elevated Sb concentrations. SRB may further influence Sb mobility by direct enzymatic Sb reduction. SRB can transform a wide variety of metalloids (As, Se and Ti), transition metals (Au, Co, Cr, Fe, Hg, Mo, Mn, Ni, Pb, Pd, Pt, Re, Rh, Tc, V, and Zn), and actinides (Pu and U) (Barton et al., 2015).Therefore, we cannot rule out the metabolic versatility of SRB in direct enzymatic Sb reduction.

5. Conclusions

In summary, microbial community was characterized and the correlation between microbial community and geochemical profiles was investigated. CCA indicated that Sb_{aq} and Sb_{exc} had a considerable impact on overall microbial community structure. Moreover, other geochemical parameters such as pH, Eh, As, sulfate, and water temperature also had significant impact on the indigenous microbial community, indicating the importance of a combination of *in situ* geochemical parameters in shaping the microbial communities. In addition, this study provided the first evidence of selective enrichment of several bacterial clades with elevated Sb in the sediment and water column. The present work provides novel knowledge of the interactions of microorganisms with Sb and other geochemical parameters, expanding our understanding of microbial metabolism of Sb. Future investigations are needed to isolate these phylotypes to enable testing of their capabilities in Sb transformation as well as to profile the metagenomics to understand the functional genes that are vital to biogeochemical Sb cycling and resistance.

Acknowledgments

This research was funded by the National Natural Science Foundation of China (41103080, 41173028), the Public Welfare Foundation of the Ministry of Water Resources of China (201501011), and the Opening Fund of State Key Laboratory of Environmental Geochemistry (SKLEG20150809). We thank Dr. Ying Huang for her suggestion and help for CCA and statistical analysis. We thank Dr. Max Haggblom, Dr. Shawn Beitel, and Dr. Dayna Schultz for thoughtful reviews of the manuscript and discussion of the topics therein.

Appendix A. Supplementary data

Supplementary data to this article can be found online at http://dx.doi.org/10.1016/j.scitotenv.2016.01.090.

References

Ashley, P., Craw, D., Graham, B., Chappell, D., 2003. Environmental mobility of antimony around mesothermal stibnite deposits, New South Wales, Australia and southern New Zealand. J. Geochem. Explor. 77, 1–14.

Barton, L.L., Tomei-Torres, F.A., Xu, H., Zocco, T., 2015. Metabolism of metals and metalloids by the sulfate-reducing bacteria. In: Saffarini, D. (Ed.), Bacteria–Metal Interactions. Springer, Gewerbestrasse, pp. 57–83.

Belzile, N., Chen, Y.-W., Filella, M., 2011. Human exposure to antimony: I. Sources and intake. Crit. Rev. Environ. Sci. Technol. 41, 1309–1373.

Bokulich, N.A., Subramanian, S., Faith, J.J., Gevers, D., Gordon, J.I., Knight, R., et al., 2013. Quality-filtering vastly improves diversity estimates from Illumina amplicon sequencing. Nat. Methods 10, 57–59.

Buanuam, J., Wennrich, R., 2010. Dynamic flow-through sequential extraction for assessment of fractional transformation and inter-element associations of arsenic in stabilized soil and sludge. J. Hazard. Mater. 184, 849–854.

Caporaso, J.G., Kuczynski, J., Stombaugh, J., Bittinger, K., Bushman, F.D., Costello, E.K., et al., 2010. QIIME allows analysis of high-throughput community sequencing data. Nat. Methods 7, 335–336.

Caporaso, J.G., Lauber, C.L., Walters, W.A., Berg-Lyons, D., Lozupone, C.A., Turnbaugh, P.J., et al., 2011. Global patterns of 16S rRNA diversity at a depth of millions of sequences per sample. Proc. Natl. Acad. Sci. U. S. A. 108, 4516–4522.

Corbisier, P., Ji, G., Nuyts, G., Mergeay, M., Silver, S., 1993. *luxAB* gene fusions with the arsenic and cadmium resistance operons of *Staphylococcus aureus* plasmid pI258. FEMS Microbiol. Lett. 110, 231–238.

Corder, G.W., Foreman, D.I., 2014. Nonparametric Statistics: a Step-by-Step Approach. second ed. John Wiley & Sons, New York.

Council of the European Communities, 1976. Council Directive of 4 May 1976 on pollution caused by certain dangerous substances discharged into the aquatic environment of the Community. Off. J. L 129, 23–29.

DeSantis, T.Z., Hugenholtz, P., Larsen, N., Rojas, M., Brodie, E.L., Keller, K., et al., 2006. Greengenes, a chimera-checked 16S rRNA gene database and workbench compatible with ARB. Appl. Environ. Microbiol. 72, 5069–5072.

Edgell, K., 1989. USEPA method study 37 SW-846 method 3050 acid digestion of sediments, sludges, and soils: US environmental protection agency. Environ. Monit. Syst. Lab.

Endo, G., Silver, S., 1995. CadC, the transcriptional regulatory protein of the cadmium resistance system of *Staphylococcus aureus* plasmid pI258. J. Bacteriol. 177, 4437–4441.

Fawcett, S.E., Jamieson, H.E., 2011. The distinction between ore processing and post-depositional transformation on the speciation of arsenic and antimony in mine waste and sediment. Chem. Geol. 283, 109–118.

Feng, R., Wei, C., Tu, S., Ding, Y., Wang, R., Guo, J., 2013. The uptake and detoxification of antimony by plants: a review. Environ. Exp. Bot. 96, 28–34.

Filella, M., 2011. Antimony interactions with heterogeneous complexants in waters, sediments and soils: a review of data obtained in bulk samples. Earth-Sci. Rev. 107, 325–341.

Filella, M., Belzile, N., Chen, Y.-W., 2002. Antimony in the environment: a review focused on natural waters: I. Occurrence. Earth Sci. Rev. 57, 125–176.

Filella, M., Belzile, N., Lett, M.-C., 2007. Antimony in the environment: a review focused on natural waters. III. Microbiota relevant interactions. Earth Sci. Rev. 80, 195–217.

Filella, M., Philippo, S., Belzile, N., Chen, Y., Quentel, F., 2009. Natural attenuation processes applying to antimony: a study in the abandoned antimony mine in Goesdorf, Luxembourg. Sci. Total Environ. 407, 6205–6216.

Finneran, K.T., Johnsen, C.V., Lovley, D.R., 2003. *Rhodoferax ferrireducens* sp. nov., a psychrotolerant, facultatively anaerobic bacterium that oxidizes acetate with the reduction of Fe (III). Int. J. Syst. Evol. Microbiol. 53, 669–673.

Fornieles, A.C., de Torres, A.G., Alonso, E.V., Cordero, M.S., Pavón, J.C., 2011. Speciation of antimony (III) and antimony (V) in seawater by flow injection solid phase extraction coupled with online hydride generation inductively coupled plasma mass spectrometry. J. Anal. At. Spectrom. 26, 1619–1626.

Fredrickson, J.K., Zachara, J.M., Kennedy, D.W., Liu, C., Duff, M.C., Hunter, D.B., et al., 2002. Influence of Mn oxides on the reduction of uranium (VI) by the metal-reducing bacterium *Shewanella putrefaciens*. Geochim. Cosmochim. Acta 66, 3247–3262.

Gault, A., Polya, D., Charnock, J., Islam, F., Lloyd, J., Chatterjee, D., 2003. Preliminary EXAFS studies of solid phase speciation of As in a West Bengali sediment. Mineral. Mag. 67, 1183–1191.

Gebel, T., 1997. Arsenic and antimony: comparative approach on mechanistic toxicology. Chem. Biol. Interact. 107, 131–144.

Ghosh, D., Bhadury, P., Routh, J., 2014. Diversity of arsenite oxidizing bacterial communities in arsenic-rich deltaic aquifers in West Bengal, India. Front. Microbiol. 5.

Giloteaux, L., Holmes, D.E., Williams, K.H., Wrighton, K.C., Wilkins, M.J., Montgomery, A.P., et al., 2012. Characterization and transcription of arsenic respiration and resistance genes during in situ uranium bioremediation. ISME J. 7, 370–383.

Haas, B.J., Gevers, D., Earl, A.M., Feldgarden, M., Ward, D.V., Giannoukos, G., et al., 2011. Chimeric 16S rRNA sequence formation and detection in Sanger and 454-pyrosequenced PCR amplicons. Genome Res. 21, 494–504.

Hamamura, N., Itai, T., Liu, Y., Reysenbach, A.L., Damdinsuren, N., Inskeep, W.P., 2014. Identification of anaerobic arsenite-oxidizing and arsenate-reducing bacteria associated with an alkaline saline lake in Khovsgol, Mongolia. Environ. Microbiol. Rep. 6, 476–482.

Hammel, W., Debus, R., Steubing, L., 2000. Mobility of antimony in soil and its availability to plants. Chemosphere 41, 1791–1798.

He, M., Yang, J., 1999. Effects of different forms of antimony on rice during the period of germination and growth and antimony concentration in rice tissue. Sci. Total Environ. 243–244, 149–155.

He, M., Wang, X., Wu, F., Fu, Z., 2012. Antimony pollution in China. Sci. Total Environ. 421, 41–50.

Heidelberg, J.F., Paulsen, I.T., Nelson, K.E., Gaidos, E.J., Nelson, W.C., Read, T.D., et al., 2002. Genome sequence of the dissimilatory metal ion-reducing bacterium *Shewanella oneidensis*. Nat. Biotechnol. 20, 1118–1123.

Huang, Y., Li, H., Rensing, C., Zhao, K., Johnstone, L., Wang, G., 2012. Genome sequence of the facultative anaerobic arsenite-oxidizing and nitrate-reducing bacterium *Acidovorax* sp. strain NO1. J. Bacteriol. 194, 1635–1636.

Jenkins, R.O., Forster, S.N., Craig, P.J., 2002. Formation of methylantimony species by an aerobic prokaryote: *Flavobacterium* sp. Arch. Microbiol. 178, 274–278.

Johnson, D.B., Hallberg, K.B., 2005. Acid mine drainage remediation options: a review. Sci. Total Environ. 338, 3–14.

Johnson, C.A., Moench, H., Wersin, P., Kugler, P., Wenger, C., 2005. Solubility of antimony and other elements in samples taken from shooting ranges. J. Environ. Qual. 34, 248–254.

Kinegam, S., Yingprasertchai, T., Tanasupawat, S., Leepipatpiboon, N., Akaracharanya, A., Kim, K.-W., 2008. Isolation and characterization of arsenite-oxidizing bacteria from arsenic-contaminated soils in Thailand. World J. Microbiol. Biotechnol. 24, 3091–3096.

Kreutz, B., Götz, F., 1984. Construction of *Staphylococcus* plasmid vector pCA43 conferring resistance to chloramphenicol, arsenate, arsenite and antimony. Gene 31, 301–304.

Krzywinski, M., Schein, J., Birol, I., Connors, J., Gascoyne, R., Horsman, D., et al., 2009. Circos: an information aesthetic for comparative genomics. Genome Res. 19, 1639–1645.

Kuczynski, J., Stombaugh, J., Walters, W.A., González, A., Caporaso, J.G., Knight, R., 2012. Using QIIME to analyze 16S rRNA gene sequences from microbial communities. Curr. Protoc. Microbiol. (1E.5.1–1E.5.20).

Lear, G., Song, B., Gault, A., Polya, D., Lloyd, J., 2007. Molecular analysis of arsenate-reducing bacteria within Cambodian sediments following amendment with acetate. Appl. Environ. Microbiol. 73, 1041–1048.

Lepš, J., Šmilauer, P., 2003. Multivariate Analysis of Ecological Data Using CANOCO. Cambridge University Press.
Li, J., Wang, Q., Zhang, S., Qin, D., Wang, G., 2013. Phylogenetic and genome analyses of antimony-oxidizing bacteria isolated from antimony mined soil. Int. Biodeterior. Biodegrad. 76, 76–80.
Lin, Y., Fan, H., Hao, X., Johnstone, L., Hu, Y., Wei, G., et al., 2012. Draft genome sequence of *Halomonas* sp. strain HAL1, a moderately halophilic arsenite-oxidizing bacterium isolated from gold-mine soil. J. Bacteriol. 194, 199–200.
Liu, C., Gorby, Y.A., Zachara, J.M., Fredrickson, J.K., Brown, C.F., 2002. Reduction kinetics of Fe (III), Co (III), U (VI), Cr (VI), and Tc (VII) in cultures of dissimilatory metal-reducing bacteria. Biotechnol. Bioeng. 80, 637–649.
Lovley, D.R., Giovannoni, S.J., White, D.C., Champine, J.E., Phillips, E., Gorby, Y.A., et al., 1993. *Geobacter metallireducens* gen. nov. sp. nov., a microorganism capable of coupling the complete oxidation of organic compounds to the reduction of iron and other metals. Arch. Microbiol. 159, 336–344.
Lovley, D.R., Holmes, D.E., Nevin, K.P., 2004. Dissimilatory Fe (III) and Mn (IV) reduction. Adv. Microb. Physiol. 49, 219–286.
Luo, J., Bai, Y., Liang, J., Qu, J., 2014. Metagenomic approach reveals variation of microbes with arsenic and antimony metabolism genes from highly contaminated soil. PLoS One 9, e108185.
Macur, R.E., Jackson, C.R., Botero, L.M., Mcdermott, T.R., Inskeep, W.P., 2004. Bacterial populations associated with the oxidation and reduction of arsenic in an unsaturated soil. Environ. Sci. Technol. 38, 104–111.
Magoč, T., Salzberg, S.L., 2011. FLASH: fast length adjustment of short reads to improve genome assemblies. Bioinformatics 27, 2957–2963.
Majzlan, J., Lalinská, B., Chovan, M., Bläß, U., Brecht, B., Göttlicher, J., et al., 2011. A mineralogical, geochemical, and microbiogical assessment of the antimony- and arsenic-rich neutral mine drainage tailings near Pezinok, Slovakia. Am. Mineral. 96, 1–13.
McBeth, J.M., Fleming, E.J., Emerson, D., 2013. The transition from freshwater to marine iron-oxidizing bacterial lineages along a salinity gradient on the Sheepscot River, Maine, USA. Environ. Microbiol. Rep. 5, 453–463.
Michalke, K., Wickenheiser, E., Mehring, M., Hirner, A., Hensel, R., 2000. Production of volatile derivatives of metal (loid) s by microflora involved in anaerobic digestion of sewage sludge. Appl. Environ. Microbiol. 66, 2791–2796.
Migon, C., Mori, C., Tian, R.C., Orsini, A., 1995. Arsenic and antimony contamination in a riverine environment affected by an abandoned realgar mine. Toxicol. Environ. Chem. 52, 221–230.
Nakamaru, Y., Tagami, K., Uchida, S., 2006. Antimony mobility in Japanese agricultural soils and the factors affecting antimony sorption behavior. Environ. Pollut. 141, 321–326.
Ning, Z., Xiao, T., Xiao, E., 2015. Antimony in the soil–plant system in an Sb mining/smelting area of Southwest China. Int. J. Phytoremediation 17, 1081–1089.
Okkenhaug, G., Zhu, Y.-G., Luo, L., Lei, M., Li, X., Mulder, J., 2011. Distribution, speciation and availability of antimony (Sb) in soils and terrestrial plants from an active Sb mining area. Environ. Pollut. 159, 2427–2434.
Pokrovsky, O., Martinez, R., Kompantzeva, E., Shirokova, L., 2014. Surface complexation of the phototrophic anoxygenic non-sulfur bacterium *Rhodopseudomonas palustris*. Chem. Geol. 383, 51–62.
Risso, C., Sun, J., Zhuang, K., Mahadevan, R., DeBoy, R., Ismail, W., et al., 2009. Genome-scale comparison and constraint-based metabolic reconstruction of the facultative anaerobic Fe (III)-reducer *Rhodoferax ferrireducens*. BMC Genomics 10, 447.
Rueda-Holgado, F., Bernalte, E., Palomo-Marin, M., Calvo-Blazquez, L., Cereceda-Balic, F., Pinilla-Gil, E., 2012. Miniaturized voltammetric stripping on screen printed gold electrodes for field determination of copper in atmospheric deposition. Talanta 101, 435–439.
Sadiq, M., 1997. Arsenic chemistry in soils: an overview of thermodynamic predictions and field observations. Water Air Soil Pollut. 93, 117–136.
Saltikov, C.W., Wildman, R.A., Newman, D.K., 2005. Expression dynamics of arsenic respiration and detoxification in *Shewanella* sp. strain ANA-3. J. Bacteriol. 187, 7390–7396.
Savonina, E.Y., Fedotov, P., Wennrich, R., 2012. Fractionation of Sb and As in soil and sludge samples using different continuous-flow extraction techniques. Anal. Bioanal. Chem. 403, 1441–1449.
Schloss, P.D., Westcott, S.L., Ryabin, T., Hall, J.R., Hartmann, M., Hollister, E.B., et al., 2009. Introducing mothur: open-source, platform-independent, community-supported software for describing and comparing microbial communities. Appl. Environ. Microbiol. 75, 7537–7541.
Schumacher, B.A., 2002. Methods for the determination of total organic carbon (TOC) in soils and sediments. Ecol. Risk Assess. Support Cent. 1–23.
Shi, Z., Cao, Z., Qin, D., Zhu, W., Wang, Q., Li, M., et al., 2013. Correlation models between environmental factors and bacterial resistance to antimony and copper. PLoS One 8, e78533.
Silver, S., Budd, K., Leahy, K., Shaw, W., Hammond, D., Novick, R., et al., 1981. Inducible plasmid-determined resistance to arsenate, arsenite, and antimony (III) in *Escherichia coli* and *Staphylococcus aureus*. J. Bacteriol. 146, 983–996.
United States Environmental Protection Agency, 1979. Toxics release inventory. Doc. 745-R-00-007. USEPA, Washington, DC, USA.
Vanden Hoven, R.N., Santini, J.M., 2004. Arsenite oxidation by the heterotroph *Hydrogenophaga* sp. str. NT-14: the arsenite oxidase and its physiological electron acceptor. BBA-Bioenerg. 1656, 148–155.
Villarroel, L.F., Miller, J.R., Lechler, P.J., Germanoski, D., 2006. Lead, zinc, and antimony contamination of the Rio Chilco–Rio Tupiza drainage system, Southern Bolivia. Environ. Geol. 51, 283–299.
Walters, W.A., Caporaso, J.G., Lauber, C.L., Berg-Lyons, D., Fierer, N., Knight, R., 2011. PrimerProspector: de novo design and taxonomic analysis of barcoded polymerase chain reaction primers. Bioinformatics 27, 1159–1161.
Wang, Q., Garrity, G.M., Tiedje, J.M., Cole, J.R., 2007. Naive Bayesian classifier for rapid assignment of rRNA sequences into the new bacterial taxonomy. Appl. Environ. Microbiol. 73, 5261–5267.
Wang, X., He, M., Xi, J., Lu, X., 2011. Antimony distribution and mobility in rivers around the world's largest antimony mine of Xikuangshan, Hunan Province, China. Microchem. J. 97, 4–11.
Wang, H., Chen, F., Mu, S., Zhang, D., Pan, X., Lee, D.-J., et al., 2013. Removal of antimony (Sb (V)) from Sb mine drainage: biological sulfate reduction and sulfide oxidation–precipitation. Bioresour. Technol. 146, 799–802.
Wenzel, W.W., Kirchbaumer, N., Prohaska, T., Stingeder, G., Lombi, E., Adriano, D.C., 2001. Arsenic fractionation in soils using an improved sequential extraction procedure. Anal. Chim. Acta 436, 309–323.
Wilson, S.C., Lockwood, P.V., Ashley, P.M., Tighe, M., 2010. The chemistry and behaviour of antimony in the soil environment with comparisons to arsenic: a critical review. Environ. Pollut. 158, 1169–1181.
Zhang, N., Wan, S., Li, L., Bi, J., Zhao, M., Ma, K., 2008. Impacts of urea N addition on soil microbial community in a semi-arid temperate steppe in northern China. Plant Soil 311, 19–28.